Double Resonance Modulation as a Standard Technique in Microwave Spectroscopy

I. Principles and Operation

Otto L. Stiefvater

School of Physical and Molecular Sciences, University College of North Wales
Bangor, Gwynedd, U.K.

(Z. Naturforsch. **30 a**, 1742–1755 [1975]; received October 6, 1975)

A versatile spectrometer with facilities for modulation by the microwave-microwave double resonance effect has been constructed for the continued evaluation of the double resonance modulation (DRM) technique. Investigation of the DR signal pattern and intensity for different modes of operation indicates that optimum results are achieved with a large frequency modulation of the pump radiation, and with one pump frequency precisely on resonance. The high sensitivity of the DRM spectrometer to the effects of not exactly resonant pump radiation leads to the occurrence of multiple double resonances (DRs) and makes double resonance double search experiments practicalliy feasible. The double resonance map is introduced as a convenient means for the presentation of DR-spectra, and miscellaneous practical aspects are reported.

I. Introduction

During the past decade microwave-microwave double resonance experiments [1–5] have become established as a help in the analysis of complex rotation spectra, and sporadic applications as well as instrumental variants have been reported from many laboratories [6]. However, as an easily practicable, and in many aspects superior alternative to the Stark effect modulation (SEM) predominantly used in microwave spectroscopy, the double resonance modulation (DRM) technique has apparently not been considered, and its systematics have therefore remained largely unexplored.

In contrast to this occasional use of double resonance (DR) as an auxiliary technique, we have employed DRM continuously over several years and tested its power on some 20 compounds [7]. As it became clear from this work that even the routine tasks of microwave spectroscopy could be handled with greater efficiency by DRM techniques, there naturally occurred a progressive reversal of the traditional roles of single resonance and DRM techniques. With the analysis of ~ 70 individual spectra by DRM spectroscopy alone, this process may be considered to have reached some degree of completion during the past few years. A coherent presentation of the developments which led from the pioneering experiments of Woods III, Ronn and Wilson [5] to our present use of DRM as a standard technique in microwave spectroscopy, might therefore be justified. Such an account also appears timely since there exists no written report of this work, while – perhaps not least as a result of a series of conference contributions [8] and subsequent work in other laboratories – the merits of this technique are beginning to be more widely appreciated.

The work which we shall report here is arranged in four parts, of which the present Part I connects directly to the results of Woods III, Ronn and Wilson in describing the simple, basic experiments that led to the subtle instrumental and operational modifications which, in turn, have permitted the later developments. For convenience and primarily reference in the following parts, the instrumental and experimental sections of Part I are preceeded by a brief outline of the fundamental features used in DRM spectroscopy, and they are followed by a description of our preferred way of presenting DRM results, along with miscellaneous features of the technique. Part II centers on the line shape and integrated intensity of DRM signals, while experimental methods for dealing with excited vibration states and non-rigid rotor effects are the main topics of Part III. The last part concerns the application of DRM methods in molecular structure determinations and, as a valuable by-product of these studies, an evaluation of DRM spectroscopy as a quantitative analytical tool.

Reprint requests to Otto L. Stiefvater, School of Physical and Molecular Sciences, University College of North Wales, *Bangor*, Gwynedd, U.K.

II. Fundamentals

This section recapitulates pertinent characteristics of double resonance and their utilisation for molecular modulation in microwave spectrometers.

a) Theory of Double Resonance [9–15]

For rotational three-level systems (Fig. 1) with two dipole-allowed transitions, e.g. $1 \longleftrightarrow 2$ and

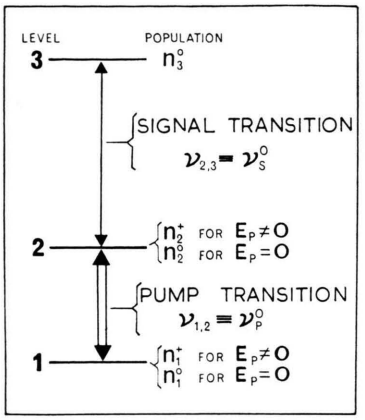

Fig. 1. Energy levels and transitions used in a typical double resonance experiment.

$2 \longleftrightarrow 3$, the 'double resonance effect' may be defined as comprising the alterations which occur in one transition (here: $2 \longleftrightarrow 3$) when the other transition which shares an energy level with the former (i.e. $1 \longleftrightarrow 2$) is simultaneously induced by high-powered 'pump' radiation. While population changes in the 'pumped' levels are perhaps the best known feature of DR, it is primarily the modification of the line shape which provides the basis for our applications. The phenomena which arise from the high-frequency Stark effect [16] will not be considered here.

Under the usual condition that the power of the 'signal' radiation which induces the transition $2 \longleftrightarrow 3$ is low enough to keep the transition rate X/π much smaller than the average collision rate $1/\tau$ (i.e. $|X| \equiv |\mu_{23} E_s|/2\hbar \ll 1/\tau$, where τ, E_s and μ_{23} are the relaxation time, the electric field vector of the signal radiation and the dipole matrix element of the signal transition, respectively) so that the population numbers of levels 2 and 3 remain unaffected by the signal radiation, the power absorbed near the resonant signal frequency $\nu_s^0 = \nu_{23}$ is given in the *absence* of pump radiation as *

$$L_{2\leftrightarrow 3}^{E_p=0}(\nu_s) = (n_2^0 - n_3^0)(\hbar/\pi\tau)|X|^2 * \quad (1)$$
$$* [\nu_s/\{(\nu_s - \nu_{23})^2 + (1/2\pi\tau)^2\}] .$$

Here, n_i^0 denotes Boltzmann population numbers, and E_p is the electric field vector of the pump radiation.

When pump radiation which represents a strong perturbation $H_p(t)$ between states 1 and 2 is applied in addition to the weak perturbation $H_s(t)$ which induces the signal transition, the three-level system is described by a time-dependent combination of stationary state wave functions,

$$\Psi_{123}(t) = C_1(t)\,\Psi_1 + C_2(t)\,\Psi_2 + C_3(t)\,\Psi_3 \quad (2)$$

and there results a simultaneous alteration of both the population numbers (hence: intensity) as well as the frequency dependence (or: line shape) of the previously unperturbed signal absorption as given by Equation (1). These two effects can be separated, however, if the signal radiation is temporarily ignored ($H_s(t) \to 0$, $C_3(t) \to$ constant, $\Psi_{123}(t) \to \Psi_{12}(t)$), and the population changes in the remaining two-level system under the influence of $H_p(t)$ alone can then be discussed independently. The result represents a reasonable approximation for the complete three-level system provided $H_p(t) \gg H_s(t)$, as is indeed the case in our applications.

a) i. Population changes. – In the presence of the strong perturbation $H_p(t)$ the wave function $\Psi_{12}(t)$ of the 'pumped' states becomes periodically dependent on the time and, for exact resonance of the pump radiation, the modulation frequency of the coefficients $C_1(t)$ and $C_2(t)$ of Eq. (2) is [9, 6e] $|Y|/2\pi = |\mu_{12} E_p|/2h$, where μ_{12} is the dipole matrix element of the pumped transition and E_p is the electric field vector of the pump radiation. This implies transitions between the pumped states at the rate $|Y|/\pi$ which in the absence of collisions or for infinite pump power would equalise the populations of these levels. However, due to the occurrence of collisions which counteract the process of saturation by exchanging molecules in the pumped levels with those in other levels that are not affected by $H_p(t)$, and hence populated according to the Boltzmann law, and due to the finite pump power available in reality, complete saturation

$$(n_1^+ = n_2^+ = (1/2)(n_1^0 + n_2^0))$$

can not be reached in practice. Instead, a balance is established between the two opposing effects and the

* The partial absorption coefficient [17] is obtained from $L_{2\leftrightarrow 3}$ by multiplication with $8\pi/3\,c\,E_s^2$.

value reached by the population of the energetically higher level is given [9, 18] in dependence of the amount of pump power and the relaxation time as

$$n_2^+(E_p,\tau) = (1/2) \quad (3\,a)$$
$$[n_1^0 + n_2^0 - (n_1^0 - n_2^0)/(1 + E_p^2\,|\mu_{12}|^2\,\tau^2/\hbar^2)]$$

where n^+ denotes population numbers in the presence of pump radiation. Accordingly, the pump radiation will increase the population of the higher pumped level at the expense of the lower level by the amount

$$\delta n_2(E_p,\tau) = -\delta n_1(E_p,\tau)$$
$$= (1/2)\,(n_1^0 - n_2^0) \quad (3\,b)$$
$$\cdot [1 - 1/(1 + E_p^2\,|\mu_{12}|^2\,\tau^2/\hbar^2)]$$

and the integrated intensity of a signal transition involving either of the pumped levels will be altered correspondingly.

a) ii. Modification of the Line Shape of the Signal Transition. – The modification of the frequency factor in Eq. (1) as a result of the application of pump radiation is obtained if the coefficients $C_i(t)$ of Eq. (2) are determined for the complete three-level system exposed to the two perturbations $H_p(t)$ and $H_s(t)$. This task is facilitated by the observation that, for large pump power and the assumed low power level of the signal radiation, the rate of transitions between the signal levels is negligible in comparison with the rate of transitions between the pumped levels ($|X| \ll |Y|$). A molecule originally thrown into state 3 by its last collision is then found [9] to possess a finite probability not only for the usual single quantum transition to level 2 but also for a double quantum transition $3 \rightarrow 1$, and vice versa. With the additional assumption that the pump power is so large that the transition rate between the pumped levels is also considerably higher than the rate of collisions [i.e. $|Y|^2\tau^2 \gg 1$ and hence $\delta n_2 = (1/2)\,(n_1^0 - n_2^0)$], the absorption ** of power near the signal frequency ν_s due to single- and double-quantum transitions is obtained for *exactly* resonant pump radiation as

$$L_{(1,2)\leftrightarrow 3}^{E_p \neq 0}(\nu_s) = [(1/2)\,(n_1^0 + n_2^0) - n_3^0]\,(\hbar/\pi\tau)\,|X|^2 * *(\nu_s/2)\,([(\nu_s - \nu_{23} - |Y|/2\pi)^2 + (1/2\pi\tau)^2]^{-1} + [(\nu_s - \nu_{23} + |Y|/2\pi)^2 + (1/2\pi\tau)^2]^{-1}). \quad (4\,a)$$

** Emission does not occur since, for experimental reasons, we prefer to choose $\nu_p < \nu_s$.

For only partial saturation

$$(0 < \delta n_2 < (1/2)\,(n_1^0 - n_2^0))$$

this becomes

$$L_{(1,2)\leftrightarrow 3}^{E_p \neq 0}(\nu_s) = [n_2^0 - n_3^0 + \delta n_2(E_p,\tau)]\,(\hbar/\pi\tau)\,|X|^2 * f(\nu_s) \quad (4\,b)$$

where $f(\nu_s)$ is the frequency dependent part of Eq. (4 a) and $\delta n_2(E_p,\tau)$ is given by Equation (3 b).

From Eq. (4 a), the pump radiation and the time-modulation of the pumped states which it entails, is seen to split the original signal transition [Eq. (1) and Fig. 2 a) into a symmetrical doublet *** [Eq. (4) and Fig. 2 b] with maxima at

$$\nu_{s\pm} = \nu_{23} \pm |Y|/2\pi \quad (5)$$

and hence with a separation $\Delta\nu_s$ which is equal to the transition rate between the pumped levels [or: twice the periodicity of $\Psi_{12}(t)$]. This splitting depends linearly on E_p and, therefore, on the square-root of the pump power density.

When the pump frequency deviates by a small amount from exact resonance the doublet described

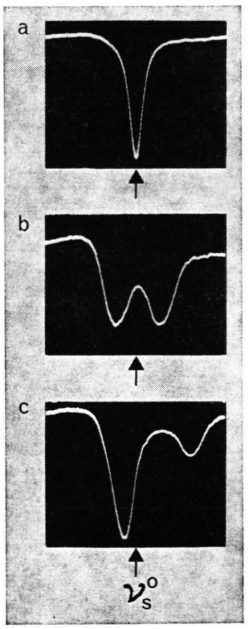

Fig. 2. Modification of an absorption line (trace **a**) into a symmetrical double (trace **b**) by exactly resonant pump radiation, and into an asymmetrical doublet (trace **c**) by slightly off-resonant pump radiation. (Molecule: propionyl fluoride [6f].)

*** Under our experimental conditions the fine structure discussed in Refs. 14 and 6h is not noticeable.

by Eq. (4) loses its symmetry both with respect to intensity and frequency displacement from $\nu_{23}=\nu_s{}^0$; while one of the components approaches ν_{23} more closely than for exact resonance of the pump radiation, the other one ('creeper') is further removed from that frequency in accordance with the approximate relation [1, 4] $\nu_{\text{creeper}}=\nu_{23}\pm(\nu_{12}-\nu_p)$, and its intensity is reduced (Figure 2 c). Since population and hence intensity changes (a – i, above) may also be transmitted to absorption lines which do not share an energy level with the pumped transition [19, 20], it is the splitting of an absorption line which provides unambiguous evidence that the signal and pump transition are coupled through a common energy level. This splitting represents therefore the basic experimental fact from which the diagnostic uses of DR derive. It also enables the modulation technique described next.

b) Double Resonance Modulation (DRM)

The observation of the splitting of an absorption line by the DR effect can become laborious when the unperturbed transition is weak. Furthermore, the utility of DR is sometimes impaired in complex spectra by overlap between different transitions and/or their Stark lobes. These practical limitations are overcome by the use of the DRM technique [5], instead of Stark effect modulation [21] with simultaneous application of continuous pump radiation [2–4].

In the DRM spectrometer the alteration of the unperturbed line shape as given by Eq. (1) into that described by Eq. (4) is produced periodically through the repetitive application and removal of the saturating power to the pump transition. As a result of the corresponding alternation between two different line shapes of the signal transition, power modulation of the signal radiation is achieved which is proportional to the difference between the power absorbed under each of the alternating conditions, and which can be monitored, as in Stark spectroscopy, by selective amplification and phase-sensitive detection at the modulation frequency of the pump radiation. The expression for the signal S in a DRM spectrometer is given, accordingly, as the difference between Eq. (4) and Eq. (1):

$$S^{\text{DRM}}(\nu_s)\propto L^{E_p\neq 0}_{(1,2)\leftrightarrow 3}(\nu_s)-L^{E_p=0}_{2\leftrightarrow 3}(\nu_s)\,. \qquad (6)$$

Since the first term in this expression describes the double resonance doublet (Fig. 2 b) which occurs

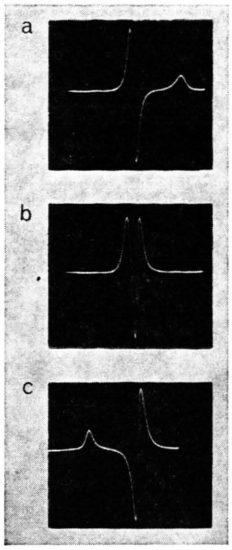

Fig. 3. Behaviour of the double resonance modulated signal as the pump frequency is tuned through the resonant pump transition. Trace a: $\nu_p<\nu_p{}^0$, trace b: $\nu_p=\nu_p{}^0$, trace c: $\nu_p>\nu_p{}^0$. (Molecule: OCS, $J=1\rightarrow 2/J=2\rightarrow 3$.)

during that half of the modulation cycle in which the pump radiation is applied, the total pattern near ν_{23} consists of three maxima and the "double resonance lobes" and the central "zero pump line" are displayed in opposite directions due to the lock-in detection (Figure 3 b).

Although DRM is seen to utilise the same technical principle as Stark effect modulation, it differs from the latter in an important aspect. In Stark spectroscopy all absorptions are modulated to a greater or lesser extent and this leads, particularly with asymmetric rotors, to dense spectra with frequent overlap between transitions or Stark components. In contrast to that, DRM is effective only on those transitions (signal) which share an energy level with a second transition near the pump frequency and, on account of the variability of the latter, it affords a means for *selective molecular modulation*. In general, therefore, no absorption will be observed at all in a DRM spectrometer for arbitrary frequency settings of the signal- and pump radiation, and for a pump frequency at or near (see Sect. IV c, below) a transition which shares an energy level with a preselected signal transition, all other absorptions in the vicinity of that signal line are eliminated. The chances for overlap between DRM signals involving different rotational energy levels of a given molecule are, therefore, minimised,

and overlap between DRM signals from different molecules is extremely unlikely. This latter feature makes for the unequalled molecular specificity of the DRM technique.

III. Instrumental

Although it is one of the main features of DRM that it eliminates the need for a high-powered squarewave generator and an absorption cell with a Stark electrode, the block diagramme of Fig. 4 shows an instrument of which the basic unit is a Hughes-Wilson [21] type SEM spectrometer. Besides the construction and use of this particular instrument for the experiments reported in this paper, a description of this 'hybrid' spectrometer appears justified not only on account of its continuing popularity in other laboratories [22], but also by the fact that large portions of it [a) and b) below] apply in full to the proper DRM spectrometer used in our later work [6g, 7b-t]. The attractive features of such an instrument for initial and exploratory DR tests are twofold. Firstly: The DR-facilities (shaded components in Fig. 4) are assembled entirely from standard waveguide components, and are grafted onto the type of SEM instrument commonly available. They can also be added to modern commercial instruments of this type, in which case a broad-banded semi-automated DRM instrument can be obtained. Secondly: As early DR work [1-5] has created the impression * that knowledge of the frequencies of potential signal and pump transitions is a prerequisite for successful DR-tests, and as no signal is observed with the DRM technique unless two interconnected resonance conditions are met simultaneously (section II-b, above), the DRM spectrometer proper (as which we define an instrument providing exclusively for modulation by the DR effect) has to appear prone to protracted failures if an unknown spectrum were to be investigated without prior examination of the normal (single resonance) spectrum. The flexibility (section c, below) of a hybrid instrument like that of Fig. 4, permitting, above all, immediate conversion to SEM spectroscopy, appears therefore preferable to the DRM spectrometer proper with an 'empty' absorption cell.

* This apparently still wide-spread pessimism is proven unfounded by the results of Sect. IV, c of this paper, and by our later work [7] which developed from these results.

a) Radiation Sources and Waveguide System

OKI klystrons with a power output of 150 mW to 800 mW are used as sources for both the pump and signal radiation. In our preferred mode of operation, which corresponds to maximum pump power in the absorption cell, the K-band radiation is fed straight into the cell, whereas the signal radiation (Q-band) is fed from a side arm via a 10 db directional coupler. It is this latter component which necessitates medium-powered ($\sim$200 mW) signal klystrons. Both sources are decoupled from the waveguide system by ferrite isolators, which are followed by the usual circuitry for manipulating microwave radiation. The propagation of K-band radiation is suppressed in the Q-band arm of the input system by a second isolator, while a waveguide filter (pass-band: 18 GHz – 27 GHz) prevents Q-band radiation from entering the K-band arm. Behind the absorption cell, a 3 db coupler delivers Q-band radiation to the signal detector which is protected from the pump radiation by a waveguide cut-off section. The amount of pump power passing through the absorption cell is monitored by a crystal which is protected from Q-band radiation by another band-pass filter. The attenuator preceeding this detector provides a load for the pump radiation and protects the crystal from excessive power.

The arrangement shown in Fig. 4 in which both radiations are fed into the cell from the same side is to be preferred, in our opinion, to the contrary design. When the two radiations are fed in from opposite ends of the cell with the signal radiation coupled out from the main line by a 10 db coupler, it is found difficult at times to operate the signal crystal at its optimum level without simultaneously causing power saturation of the signal transition. This difficulty could be by-passed, of course, if a 3 db coupler was used instead of the 10 db of Fig. 4, but a loss of up to 50% of the pump power has then to be accepted. In situations where such a loss is tolerable (or when couplers with a large transfer [23] are available) the pump klystron can be switched to the side arm of the input system. This has the advantage that the transmission of the signal radiation, which is then fed straight into the cell, becomes more broadbanded than in the arrangement of Figure 4. The disposition of components for separating the two radiations after they emerge from the absorption cell has been found less critical. The cut-off and signal detector (Q-band) can be switched to the

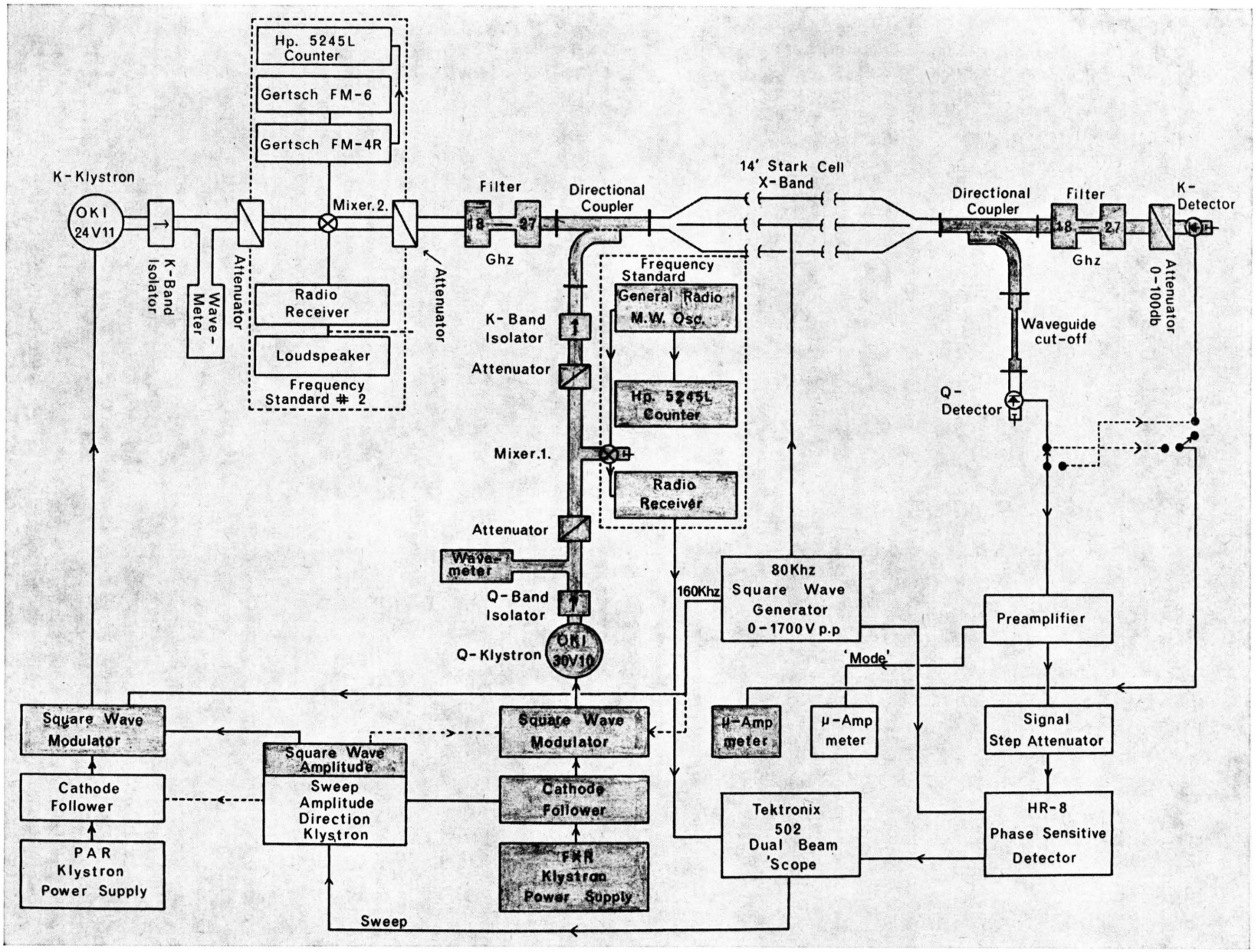

Fig. 4. Block diagramme of hybrid spectrometer. The shaded components are the additions for DR-experiments to a conventional Stark effect spectrometer.

straight arm of the 3 db coupler, with a corresponding shift of the filter and pump monitor crystal to the side arm, without appreciable deterioriation in the overall performance of the system.

b) Modulation

The functional outline of DRM in section II-b above implies complete power modulation of the pump radiation, and the successful operation of a DRM spectrometer employing this principle of modulation has been reported [24a] for pump frequencies in X-band. At higher pump frequencies, however, the non-ideal performance of waveguide filters and the presence of auxiliary crystals, which entails possibilities for the mixing of signal and pump radiation and/or the generation of harmonics, render increasingly difficult the suppression of power-modulated pump radiation at the signal detector to a level sufficiently lower than the power modulation of the signal radiation produced genuinely by the DR-effect. For pump frequencies in K-band which may approach the signal frequency to within less than 1 GHz, we have found it expedient to avoid power modulation of the pump radiation altogether if the sensitivity of the instrument is not to be impaired [6g]. In accordance with the original suggestion [5] we therefore approximate the 'zero-pump' condition by periodically pulling the frequency away from the resonant pump transition by as large an amount as is compatible with the simultaneous requirement of minimal power modulation. Technically, this is accomplished through the application of a squarewave with adjustable amplitude (0 – 60 V) to the repeller of the pump klystron.

c) Electronics

The electrical supplies and modulation units are arranged symmetrically for the signal and pump klystron. Provision for sawtooth and/or squarewave modulation of either klystron results in considerable flexibility of the system. When operated as a SEM spectrometer with the pump radiation attenuated and the signal klystron swept, normal spectroscopy can be performed in either frequency band. This allows, for instance, tentative pump transitions to be selected immediately before a DR experiment, or accurate frequency measurements to be taken immediately after such an experiment. The DR experiment itself can be performed either on Stark modulated lines by the application of CW pump radiation or, after the removal of the Stark field and the application of the modulating squarewave to the repeller of the pump klystron, by the DRM technique. By inspection of the frequency swept mode of the pump klystron (sawtooth modulation) adjustments can be made to minimise the power modulation which normally accompanies the frequency modulation of the pump radiation. Finally, with appropriate preselection of filters and cut-off sections at the detector end, and provided that sufficient power is available from the Q-band klystron, the role of the signal and pump radiation can be interchanged without re-arrangement of the waveguide system or the radiation sources. Numerous experiments of this type have shown that leakage of pump radiation through the band-pass filters greatly impairs the performance of the system when operated in the DRM mode with $\nu_p > \nu_s$. Accordingly, we always choose the transition at the lower frequency as the pump transition in DRM spectroscopy.

IV. Experiments

The experiments of this section were carried out in order to establish an efficient and reliable mode of operation for the DRM spectrometer through maximum signal intensity with optimum definition of signal and pump frequency.

a) Signal Pattern in Dependence of the Modulation Depth of the Pump Radiation

Squarewave frequency modulation of the pump radiation implies the presence of two discrete pump frequencies in alternate halves of the modulation cycle and, since both these pump frequencies will normally give rise to a detectable DR-effect (Sect. c), different signal patterns and intensities are to be expected when the modulation depth $\Delta\nu_p$ and/or the relative position of the two pump frequencies with respect to the resonant pump frequency ν_p^0 are varied. If a 'small' modulation depth of less than ten times the (unsaturated) line width of the pump transition is used, the 'zero-pump' condition is not even approximately met in either half of the modulation cycle. The DRM signal consists, therefore, of four maxima with pairs of positive and negative peaks (Figure 5 a). These pairs represent the DR doublets which arise from each of the two pump frequencies. The 'quadruplet' assumes a symmetrical

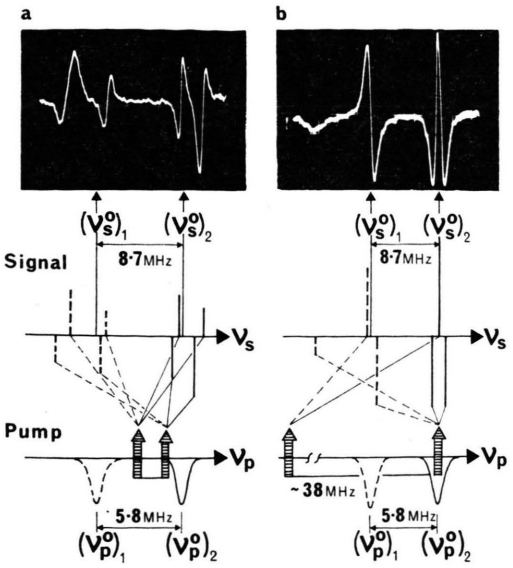

Fig. 5. Simplification of the DR-signal pattern from a quadruplet to a triplet through 'on-off' modulation with a 'large' modulation depth. Trace **a**: symmetrical modulation, trace **b**: on-off modulation. (Signals: $J=1\rightarrow 2/J=2\rightarrow 2$ of $^{16}O^{13}C^{32}S$ and $^{16}O^{12}C^{32}S$, $v_1=1$.)

frequency pattern and intensity distribution if the pump frequencies are displaced by equal amounts from $\nu_p{}^0$, provided that equal pump power is present at both frequencies. Under these conditions (which can only be checked if $\nu_p{}^0$ is known in advance and if the power modulation of the pump radiation is monitored (see Ref. 6 g) the frequency of the unperturbed signal transition corresponds to the center of the quadruplet and the frequency of the resonant pump transition is defined as the average of the two pump frequencies that are actually present. While this mode of operation can still be quite successful in strong spectra with isolated absorptions, it tends to lead into difficulties when applied in weak and dense spectra: the outermost components of the quadruplet are then frequently lost in the noise so that only an apparently differentiated signal remains. This, however, is easily overlooked, particularly on a sloping base line which results mostly from leakage of pump radiation to the signal detector. As an added disadvantage of this mode of operation absorption frequencies have normally to be remeasured under Stark modulation because of their poor definition in DRM.

While still adhering to frequency modulation of the pump radiation we have been able to remedy much of the described difficulties by increasing the modulation depth of the pump radiation to twenty to fifty times the line width. For such a 'large' modulation depth the 'zero-pump' condition is approximated closely ($\sim 95\%$, see Fig. 7) during one half of the modulation cycle. This results in the simplification of the signal pattern from a quadruplet to a triplet. When neither pump frequency coincides with $\nu_p{}^0$ this triplet (Fig. 3 a, 3 c) is composed of an asymmetrical doublet which represents the split absorption due to that pump frequency which is nearer to $\nu_p{}^0$ and a central peak close to the unperturbed signal frequency $\nu_s{}^0$. This 'zero-pump' line is the remainder of the second DR-doublet of which one component is displaced by a large amount and hence practically removed. From this, a large frequency modulation of the pump radiation is seen to produce nearly the same DRM absorption pattern as would be expected for complete power modulation. The traces of Fig. 3 were, in fact, obtained with a large frequency modulation of the pump radiation. Coincidence of the pump frequency with the resonant pump transition is indicated in this mode of operation by the occurrence of a symmetrical ** DR doublet with the zero-pump line located in the middle of the doublet components (Fig. 3 b and signal on the right in Figure 5 b). The zero-pump line which would occur at $\nu_s{}^0$ precisely for an infinite modulation depth only, defines, in our experience, the unperturbed signal frequency to better than ± 0.2 MHz and the uncertainty in the determination of $\nu_p{}^0$ has been found to be ± 0.5 MHz at the most.

The improvements in signal definition through a large modulation depth of the pump frequency are illustrated in Figure 5. They are particularly useful in dense spectra with adjacent DRs due to excited vibration states or isotopic species, and in experiments in which the spectra have not been investigated previously by single resonance techniques. It is this good definition of absorption frequencies that has allowed us to analyse spectra by DRM only, i.e. without recurrence to Stark spectroscopy. Both oscilloscope traces of Fig. 5 are augmented by sketches which are meant to indicate the origin of the various peaks. It should be noted that, while in Fig. 5 b the upper of the two pump frequencies is easily recognised as being on resonance with the transition connected with the signal line on the right (OCS, $v_1=1$), the pump frequencies are not symmetrical

** The asymmetry of the doublet as predicted in figure 6 of ref. 14 is again omitted here.

to either pump transition in Fig. 5 a, although the two signal quadruplets do not appear grossly unbalanced.

b) Signal Intensity in Dependence of the Modulation Depth and Modulation Scheme

Since the success of DR-experiments depends often critically on the signal amplitude we considered it worthwhile to investigate quantitatively how the signal amplitude varies with the modulation depth $\Delta\nu_p$ for the two possible modulation schemes.

In the previously recommended [5] 'symmetrical' modulation scheme the pump klystron is adjusted so that the average of the two modulated frequencies coincides with ν_p^0. With this scheme the intensity of the symmetrical quadruplet is found to increase at first with $\Delta\nu_p$ but then, after passing through an optimum value, to decay for larger values of $\Delta\nu_p$. The initial increase is explained as the result of the removal of overlap between the inner and outer components of the quadruplet. The subsequent decay stems primarily from the decreasing efficiency of the pump radiation due to the growing displacement of both pump frequencies from ν_p^0. As a result of this displacement, the overlap and partial cancellation between the two central peaks of the signal pattern increases, while the outer signal components are being further removed from ν_s^0 and fade out in intensity. The value of the optimum modulation depth for the symmetrical scheme is, accordingly, dependent on the power and efficiency of the pump radiation as well as on the gas pressure. It is, therefore, not normally known in advance.

In the alternative scheme of 'on-off' modulation, one of the pump frequencies is placed precisely 'on' the pump transition for one half of the modulation period and pulled 'off' during the other one. If one starts again with $\Delta\nu_p = 0$, an asymmetrical quadruplet appears first in this scheme. As the modulation depth is increased the signal changes from the quadruplet to the triplet pattern and its intensity rises quickly to a constant value while the symmetry of the triplet keeps improving. The increase and later constancy of the intensity is due to the removal of the overlap described above while the improvement in symmetry has to be ascribed to the reduction of the effects from the off-resonant pump frequency.

The quantitative results of these experiments are shown in Figure 6. The intensity curves which are normalised to the strongest signal that was obtained,

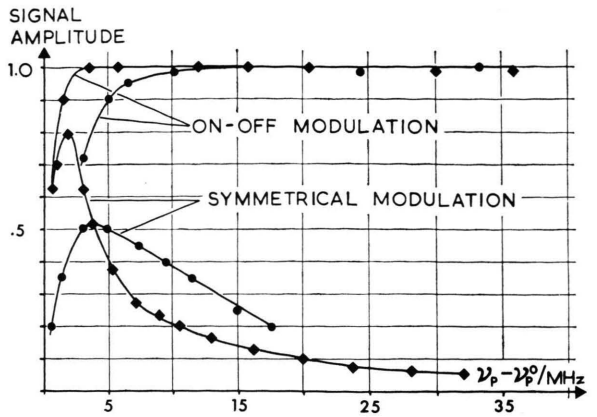

Fig. 6. Amplitude of DR-modulated signals in dependence of the modulation scheme and the modulation depth. (◆: measurements of OCS, ●: measurements on propionyl fluoride [6f].)

show clearly that for optimum signal intensity it is expedient to operate with a 'large' modulation depth in the 'on-off' scheme.

c) Signal Amplitude for Not Exactly Resonant Pump Radiation

As is easily verified from Figs. 3 a, 3 c and 5, and in agreement with theory, a detectable DR-effect occurs when the pump frequency lies well outside the (unsaturated) line width of the pump transition. This can also be inferred from the experiments with the symmetrical modulation scheme (Sect. b, above) since the signal observed in that case is entirely due to off-resonant pump radiation. These effects are less obvious in DR experiments with CW pump radiation and it was believed therefore, at the outset of our experiments, that a DR effect would become unobservable when the pump frequency deviates by more than ten times the line width from the resonant pump transition.

In contrast to the experiments with CW pump radiation, there are two signal components near ν_s^0 in the DRM spectrometer and these represent, as has been explained and illustrated above, one component from each of the DR doublets that are produced by each of the two alternating, non-resonant pump frequencies. As a result of the large frequency modulation with a corresponding difference in effectiveness of the two pump frequencies, these two absorptions are displaced from ν_s^0 by slightly different amounts and do not exactly overlap and cancel. Accordingly, the total signal near ν_s^0 due to non-resonant pump

radiation has the appearance of a differentiated absorption line (Fig. 3 and 5) but is, in fact, the unbalanced part ot two slightly displaced absorptions with a phase difference of 180°. The DRM spectrometer may, therefore, be thought of as containing a discriminator circuit which transforms the small difference between two frequency displacements from ν_s^0 into an easily noticeable signal. This feature makes the instrument very sensitive to the small DR effects from non-resonant pump radiation. Since this high sensitivity would be likely, on the other hand, to cause some uncertainty in the interpretation of DR experiments, we have examined the signal amplitude as function of the difference $\nu_p - \nu_p^0$ between the resonant pump frequency and that component of the pump radiation which is closer to ν_p^0. These experiments were first (1966) conducted on the instrument of Fig. 4 and later (1968) repeated on the DRM spectrometer of Ref. [6g]. The results were in good agreement with each other and are summarised in Figure 7. A modulation depth of 30 MHz to 50 MHz was used in these experiments and, in agreement with the qualitative interpretation, a slight reduction in signal amplitude was noticeable for a reduced modulation depth whereas an increase can be observed when the pump power at the two frequencies is grossly unbalanced.

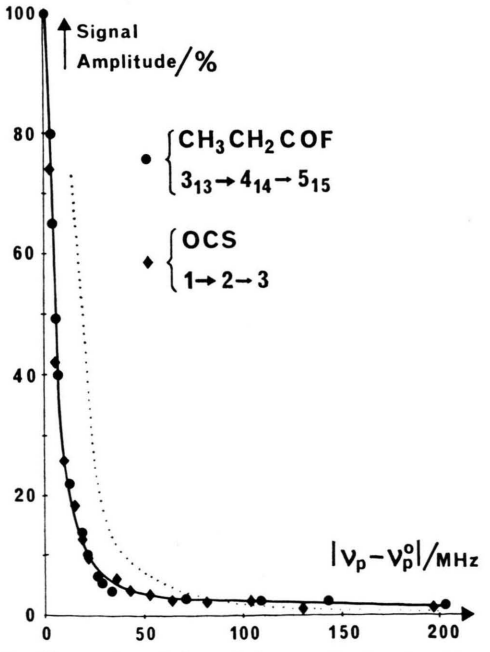

Fig. 7. Observed variation of the amplitude of a DR-modulated signal for not exactly resonant pump radiation. The dotted curve is that calculated by Flynn [25].

Some support for the proposed explanation of the high sensitivity of DRM to off-resonant pump radiation is found in theoretical work [25] which quantifies the idea of two slightly displaced absorptions. However, as may be seen from Fig. 7 which incorporates calculated [25] signal intensities (dotted curve, 250 mW pump power), there occurs a discrepancy between calculation and experiment for pump frequencies which deviate by more than 50 – 100 MHz from ν_p^0. The observed signal amplitude remains larger in this range than the calculated values. This effect has been explained [26] as the result of the high-frequency Stark effect [16] caused by the non-resonant pump radiation.

Two consequences of pre-eminent practical importance follow from the detectability of DRs for off-resonant pump radiation:

i. Multiple DRs ***. – If several pump transitions occur in the frequency-range subtending the response curve (Fig. 7), their connected signal transitions will be modulated simultaneously to a greater or lesser extent and they can, therefore, be located approximately by a scan through the signal range without adjustment of the pump frequency to each respective exact resonance point. Figure 5 gives a trivial example of this feature which provides an efficient method for the quick location of signal transitions in the case of vibrational satellite spectra (Part III).

ii. Double search. – Experiments in which neither the signal nor the pump transition are known in advance are very tedious when close coincidence of the pump frequency with the pump transition is required as, for example, for CW pump radiation. On account of the described sensitivity to off-resonant pump radiation in combination with the selective modulation (Sect. II-b), the DRM technique makes feasible such double search experiments and, relying entirely on the off-resonance effect, one can successfully attack spectra without prior experimental knowledge of the transition frequencies in the signal or pump range. Our procedure for such experiments consists in shifting the pump frequency through a predetermined range in steps of, typically, 50 MHz while the signal range is being searched for each setting of ν_p. Unless the signal and/or pump frequency deviate by several hundred MHz from

*** We exclude from this definition the trivial case in which several signals are connected to the *same* pump transition (see Section V).

their expected value, not more than three or four signal scans are normally required before the derivative-shaped signal can be located and, after tuning of the pump frequency to exact resonance, can be measured exactly.

V. Presentation of Double Resonance Spectra

In complex rotation spectra, the number of pairs of transitions with a common energy level is comparable with the number of transitions in the single resonance spectrum. In the ground state of the predominant conformer of iso-butyryl fluoride [7d], for example, there are about 170 transitions (with $J \leqq 10$ and a variation in relative intensity by a factor less than 30 in the frequency range from 15 GHz to 40 GHz) with about 450 DR-connections between them. This large number of DRs arises because individual pump transitions frequently share an energy level with more than one, and sometimes with up to twelve other transitions. For efficient use of the DRM technique it is desirable in such circumstances to have a means of presentation which gives an adequate picture of the entire two-dimensional spectrum and which allows the quick identification of predictable or previously observed DRs. A tabular presentation is useful for that purpose for spectra which are dominated by series of Q-branch transition [6g]. Successive members of a series, e.g. $J_{2,J-2} \rightarrow J_{3,J-3}$, are listed in a column and different series with a common energy level with the first one, e.g. $J_{1,J-1} \rightarrow J_{2,J-2}$ and $J_{3,J-3} \rightarrow J_{4,J-4}$ for a b-type spectrum, are listed in adjacent columns to the right and left, respectively. In the resulting table each transition will then be connected by DR to the adjacent ones in the same row. This scheme can also be applied for spectra dominated by a- or c-type R-branch transitions if the transitions belonging to the same value of $J \rightarrow J+1$ are listed in adjacent columns so that the relevant K quantum numbers [27] are constant in each row.

Although these tabulations have been found useful in the overall planning of DR investigations, these simple schemes become inadequate when transitions with different values for ΔJ are to be incorporated or when there are more than one non-zero dipole component in a molecule. It then becomes necessary to compile an ordered list of signals which are connected by DR with each potential pump transition within a given frequency range. Such a list is present-

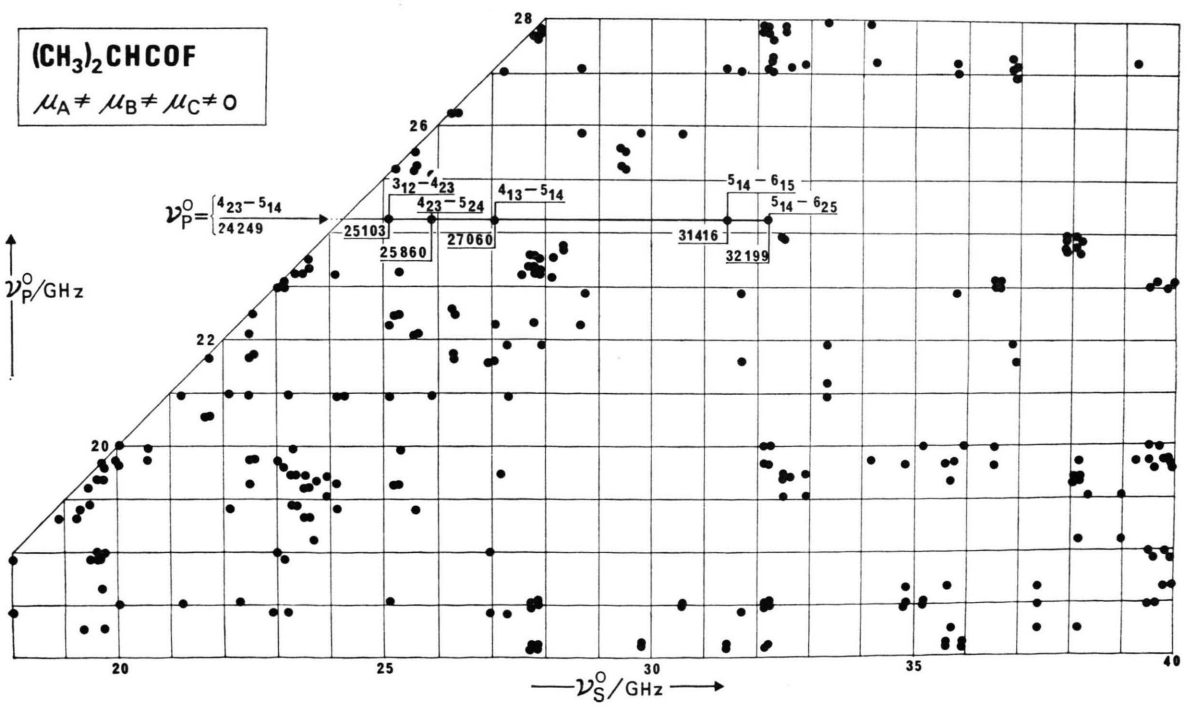

Fig. 8. 'Double Resonance Map' of iso-butyryl fluoride [7d]. Each point symbolises a combination of pump and signal frequency for which the DR-effect occurs.

ed in diagrammatic form in figure 8 and will be referred to as double resonance map. The pump frequency is plotted along the ordinate and the signal frequency along the abscissa so that the location of a particular DR signal is represented by a point at the intersection of the corresponding pump and signal frequency. For example, when the transition $4_{23} \rightarrow 5_{14} = 24{,}249$ MHz in iso-butyryl fluoride is pumped, a signal can be observed at 25,103 MHz $= 3_{12} \rightarrow 4_{23}$, but also at 25,860 MHz $= 4_{23} \rightarrow 5_{24}$, 27,060 MHz $= 4_{13} \rightarrow 5_{14}$, 31,416 MHz $= 5_{14} \rightarrow 6_{15}$ and at 32,199 MHz $= 5_{14} \rightarrow 6_{25}$. Each point in this map has a counterpart which corresponds to an interchange of signal and pump frequency and which would be located symmetrically to the line $\nu_p = \nu_s$. These points are omitted from the map, and this reflects our preferential mode of operation in which the transition at the lower frequency is chosen as the pump transition.

In our experience DR-maps have proven invaluable as an appropriate and convenient presentation of the two-dimensional spectrum, especially since they also reveal characteristic features which facilitate the analysis of spectra. Unfortunately, they can not do justice to the high resolution of microwave spectroscopy if they are extended over as large a frequency range as in Fig. 8, nor is there an easy way of incorporating the relative intensities of signals in this map.

VI. Miscellaneous

This final section is concerned with some minor aspects of DRM and with experimental details which have emerged in the operation of the instrument of Fig. 4 and of the DRM spectrometer proper which has been described in Ref. [6g]. Besides the absorption cell the latter instrument differs from that of section III above through facilities for the stabilisation of the frequency modulated pump radiation and for monitoring the undesirable power modulation of the pump radiation.

a) Sensitivity of DRM

Large enhancement of absorption signals by the use of DR have been observed [2, 28] for special cases in which a very weak transition shares an energy level with a strong transition. However, in the normal situation of connected transitions with comparable intensities it is found [14, 29] that, for identical dimensions of the absorption cell, the signal intensity does not change markedly when Stark effect modulation is replaced by DRM. Improvements in signal strength have to be sought, therefore, primarily through special instrumental features. Chief among these is the possibility to use longer absorption cells [5] than is feasible in Stark spectroscopy and, since no Stark electrode is present in the DRM cell, losses are normally reduced despite the increased cell length. It is advisable, in addition, to make more efficient use of the limited pump power which is normally available through the use of waveguide with a smaller cross-section [2] than the conventional X-band cell. These aspects were taken into account in the construction of the DRM cell of Ref. [6g] (cell dimensions: $10.7\text{ mm} \times 4.3\text{ mm} \times 21.8 \times 10^3\text{ mm}$) and, using the same detection system, we observe an increase in sensitivity of about one order of magnitude over the Stark modulated spectrometer with a conventional cell length of 4 meters.

b) Frequency Measurements

The measurement of absorption frequencies by DRM includes the subjective judgement of the symmetry of the triplet pattern and this entails corresponding uncertainties, particularly in ν_p^0. In typical cases it is found, for example, that a deviation of ± 0.2 MHz of ν_p from ν_p^0 does not affect the symmetry of the signal by an easily discernable amount. While systematic errors in the signal and pump frequency due to the subtle intrinsic asymmetry [14] of the DRM signal are negligible for a large modulation depth (section IV), additional uncertainties would result from the variation of signal power across the triplet pattern and from non-linearity of the sweep. In our normal mode of operation with free-running, frequency-swept signal klystrons and oscilloscope display of DRM signals, we do not achieve, therefore, the same accuracy in DRM as in Stark spectroscopy for individual transition frequencies. However, by using a sufficiently large number of transitions in least squares procedures and by including preferably low-J transitions which are strongly dependent on the rotational constants and which are identified unambigously by DRM, we are normally able to obtain rotational constants with the same precision as in Stark spectroscopy.

c) Phase Inversion of the DRM Signal

As a result of the frequency modulation of the pump radiation every DRM signal assumes the symmetrical triplet pattern twice if the pump klystron is tuned past ν_p^0 by more than the modulation depth. The two resonant signals correspond to coincidence of the upper or lower modulated pump

frequency with ν_p^0 and they differ, accordingly, only by a phase shift of π (inversion of signal). To eliminate the possibility of confusion and the necessity to produce every signal twice in order to determine ν_p^0 unambiguously, we find it convenient to adjust the reference phase always so that the zero-pump line points downwards, as in Fig. 3 b, for $\nu_p^{lower} = \nu_p^0$, and upwards, as in Fig. 5 b, for $\nu_p^{upper} = \nu_p^0$. This phase inversion is conveniently used as a test to distinguish very weak DRM signals from mere reflections, and it also provides for improvements in the determination of ν_p^0 through two independent measurements in cases where this is desirable.

d) Interference from Adjacent DRs

From Sect. II b it is clear that the proximity or even exact coincidence of two signal transitions (pump transitions) does not cause overlap in DRM if the respective pump transitions (signal transitions) are well separated in frequency. Interference can arise, however, when the frequencies of the two signals as well as the frequencies of their respective pump transitions both differ by less than ~ 5 MHz. This situation arises quite often when the pure rotational transitions are split into several components by, for example, internal motions or nuclear quadrupole coupling. To unravel the complicated signal pattern which can result in such cases (Fig. 9 a) and which would prevent the precise determination of corresponding signal and pump transitions, we use the following procedure: First, the pump frequency is de-tuned from the apparent ν_p^0 and the frequencies of the derivative-shaped signals (Fig. 9 b) are measured. The pump frequency is then brought back towards resonance, but now overlap is reduced through the attenuation of the pump power until the DR-lobes of each signal nearly coalesce. Through fine tuning of ν_p each of the 'undermodulated' signals is then symmetrized in turn (Fig. 9 c and 9 d) and ν_p^0 is determined while ν_s^0 is re-measured for each component. For improved accuracy the routine is finally repeated with the other modulated frequency. The procedure described here fails, for obvious reasons, for very weak and very close DRs (separation less than 2 MHz in signal and pump frequency) or when the adjacent DRs differ greatly in intensity. It then becomes necessary to select a different pump or signal transition with larger separations between its components. In heavily asymmetric rotor spectra this is frequently possible (compare Figure 8).

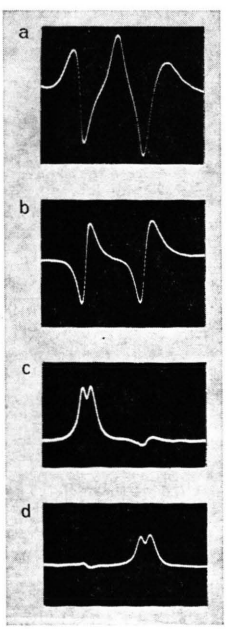

Fig. 9. Resolution of adjacent DR-signals through reduction of the pump power. Molecule: isoxazole [7p].

e) Insufficient Pump Power, Collision Induced Transitions

The splitting of the DR-doublet can become very small either because of insufficient pump power (Fig. 10 b) or because of a small line strength of the pump transition. When the population changes outlined in section II a lead to an increase of the integrated intensity of the signal transition, the zero-pump line is largely (Fig. 10 b) or completely (Fig. 10 c) extinguished by the nearly coalescing DR-lobes, and the triplet pattern of DRM signals (Fig. 10 a) degenerates into that of an ordinary absorption line (Figure 10 c). Since the opposite behaviour, in which the zero-pump line extinguishes

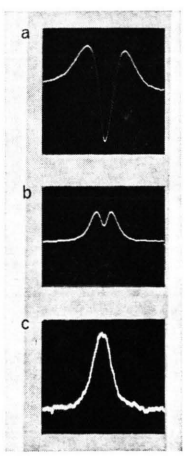

Fig. 10. 'Undermodulation' of a DR-signal as a result of small pump power. Molecule: propionic acid [7b].

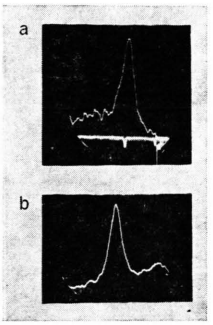

Fig. 11. Collision-induced transitions in propionyl fluoride [6f].

the DR-lobes, is also possible (Part II) the phase convention given under 3. above becomes inadequate in such cases and the correct $\nu_p{}^0$ has to be determined by a phase inversion experiment. – It may be mentioned in this context that the undermodulated DRM signal displays a similar shape as signals due to collision-induced transitions [19, 20]. We have observed this type of signals (Fig. 11) in several molecules [6f, 7] with a considerable number of internal degrees of freedom. This implies, as has been confirmed recently [30], that the occurrence of relaxation lines should not be ruled out entirely for larger molecules.

Acknowledgements

The author wishes to record his sincere gratitude to Professors E. Bright Wilson, Jr. and J. Sheridan who have provided the instrumental facilities for this work.

[1] A. Battaglia, A. Gozzini, and E. Polacco, Nuovo Cim. **14**, 1076 [1959].
[2] T. Yajima and K. Shimoda, J. Phys. Soc. Japan **15**, 1968 [1960].
[3] T. Yajima, J. Phys. Soc. Japan **16**, 1709 [1961].
[4] A. P. Cox, G. W. Flynn, and E. B. Wilson, Jr., J. Chem. Phys. **42**, 3094 [1965].
[5] R. C. Woods IIII, A. M. Ronn, and E. B. Wilson, Jr., Rev. Sci. Instrum. **37**, 927 [1966].
[6] For example: a) J. Messelyn and R. Wertheimer, C. R. Acad. Sci. Paris **258**, 4473 [1964]; b) M. L. Unland, V. Weiss, and W. H. Flygare, J. Chem. Phys. **42**, 2138 [1965]; c) R. C. Woods III, J. Chem. Phys. **46**, 4789 [1967]; d) J. Martins and E. B. Wilson, Jr., J. Mol. Spectrosc. **26**, 416 [1968]; e) T. Oka, Can. J. Phys. **47**, 2343 [1969]; f) O. L. Stiefvater and E. B. Wilson, Jr., J. Chem. Phys. **50**, 5385 [1969]; g) O. L. Stiefvater, H. Jones, and J. Sheridan, Spectrochim. Acta **26 A**, 825 [1969]; h) J. Demaison, G. Roussy, J. Rivail, and J. Sartreaux, J. Chim. Physique **67**, 899 [1970]; i) P. J. Seibt, J. Chem. Phys. **57**, 1343 [1972].
[7] These are: a) Propionyl fluoride (ref. 6 f); b) propionic acid (J. Chem. Phys. **62**, 233 and 244 [1975]); c) isobutyraldehyde (ref. 8 d); d) isobutyryl fluoride (ref. 8 c); e) isobutyric acid (ref. 8 e); f) cyclopropane carboxylic acid (ref. 8 c); g) trifluoroethylene (unpublished); h) bromoacetylene (H. Jones, O. L. Stiefvater, and J. Sheridan, unpublished); i) 1,2,3-triazole (ref. 6 g); j) isopropyl fluoride (J. H. Griffith, N. L. Owen, and J. Sheridan, J. Chem. Soc., Faraday II **69**, 1359 [1973]); k) 3-methyl isothiazole (unpublished); l)–o) propionaldehyde, propionyl chloride, dimethyl sulfide and methylene chloride (ref. 29); p) isoxazole (O. L. Stiefvater, P. Nösberger, and J. Sheridan, Chem. Phys. **9**, 435 [1975]); q) isothiazole (unpublished); r) 1,2,3-thiadiazole (in press); s) 2,6-difluoropyridine (in press); t) 1,2,4-thiadiazole (unpublished).
[8] O. L. Stiefvater: a) 1st Colloquium on High Resolution Molecular Spectroscopy, Dijon, France, 1969; b) 1st European Microwave Spectroscopy Conference, Bangor, U.K., 1970, Paper B1–3; c) 2nd Coll. on High Res. Mol. Spectrosc., Dijon, France, 1971, Lecture C; d) ibidem, Paper D-7; e) 4th Austin Symposium on Gas Phase Molecular Structure, Austin, Texas, 1972, Paper W6; f) 3rd Coll. on High Res. Mol. Spectrosc., Tours, France, 1973, Paper C-7; g) 5th Austin Symp. on Gas Phase Mol. Structure, Austin, Texas, 1974, Paper M5; h) 3rd Europ. Microwave Spectrosc. Conference, Venice, Italy, 1974, Paper C9.
[9] A. Javan, Phys. Rev. **107**, 1579 [1957].
[10] A. DiGiacomo, Nuovo Cim. **14**, 1082 [1959].
[11] T. Yajima, J. Phys. Soc. Japan **16**, 1594 [1961].
[12] H. W. DeWijn, Physica **31**, 1557 [1965].
[13] B. Macke, J. Messelyn, and R. Wertheimer, J. Phys. **27**, 579 [1966].
[14] G. W. Flynn, J. Mol. Spectrosc. **28**, 1 [1968].
[15] J. Legrand, B. Macke, J. Messelyn, and R. Wertheimer, Rev. Phys. Appl. **3**, 237 [1968].
[16] S. H. Autler and C. H. Townes, Phys. Rev. **100**, 703 [1955].
[17] C. H. Townes and A. L. Schawlow, Microwave Spectroscopy, McGraw-Hill Book Company, Inc., New York 1955.
[18] R. Karplus and J. Schwinger, Phys. Rev. **73**, 1020 [1948].
[19] T. Oka, a) J. Chem. Phys. **45**, 754 [1966]; b) ibid. **47**, 13 [1967]; c) ibid. **47**, 4852 [1967]; d) ibid. **48**, 4919 [1968]; ibid. **49**, 3135 [1968]; f) R. M. Lees and T. Oka, J. Chem. Phys. **51**, 3027 [1969]; g) D. W. Daly and T. Oka, ibid. **53**, 3272 [1970].
[20] a) A. M. Ronn and E. B. Wilson, Jr., J. Chem. Phys. **46**, 3262 [1967]; b) R. G. Gordon, P. E. Larsen, C. H. Thomas, and E. B. Wilson, Jr., J. Chem. Phys. **50**, 1388 [1969].
[21] R. H. Hughes and E. B. Wilson, Jr., Phys. Rev. **71**, 5621 [1947].
[22] For example: R. Pearson, Jr., A. Choplin, V. W. Laurie, and J. Schwartz, J. Chem. Phys. **62**, 2949 [1975].
[23] A. F. Harvey, Microwave Engineering, Academic Press, London 1963.
[24] a) H. D. Rudolph, H. Dreizler, and U. Andresen, Z. Naturforsch. **26 a**, 233 [1971]; b) U. Andresen and H. D. Rudolph, ibid. **26 a**, 320 [1971].
[25] G. W. Flynn, J. Mol. Spectrosc. **43**, 353 [1972].
[26] a) P. Glorieux, J. Legrand, B. Macke, and J. Messelyn, J. Quant. Spectrosc. Rad. Transf. **12**, 731 [1972]; b) B. Macke and P. Glorieux, J. Mol. Spectrosc. **43**, 353 [1972].
[27] G. W. King, R. M. Hainer, and P. C. Cross, J. Chem. Phys. **11**, 27 [1943].
[28] T. Oka, J. Chem. Phys. **45**, 752 [1966].
[29] R. J. Volpicelli, O. L. Stiefvater, and G. W. Flynn, NASA Contract Report, CR 967 [1967], Chem. Abs. 1968, 69, 24387g.
[30] J. B. Cohen and E. B. Wilson, Jr., J. Chem. Phys. **58**, 456 [1973].